Journal of Cleaner Production 476 (2024) 143758

Contents lists available at ScienceDirect

Journal of Cleaner Production

journal homepage: www.elsevier.com/locate/jclepro

Investigation of mixed long-term nonstationary trends in global wave energy systems

Seongho Ahn [a,*], Vincent S. Neary [b]

[a] Department of Civil Engineering, Jeju National University, Jeju, 63243, South Korea
[b] Water Power Technologies, Sandia National Laboratories, Albuquerque, NM, 87123, USA

ARTICLE INFO

Handling Editor: Mingzhou Jin

Keywords:
Wave climate change
Wave energy trend
Wave energy system
Nonstationary wave climate

ABSTRACT

The long-term historical trends in global wave energy systems are investigated using 42-year wave reanalysis from 1979 to 2020. In addition to the historical trend of omnidirectional wave power, trends of period-resolved and period-directionally resolved wave energy systems are estimated using spectral partitioned wave parameters and linked to commensurate trends in the historical wind speed. The present study shows that opposing trends in distinct wave energy systems offset each other in many oceans, e.g., the equatorial Pacific Ocean, North Atlantic Ocean, and Indian Ocean, where shorter period waves (<11 s) have decreased while the longer period waves (11–15 s) have increased. These mixed trends in the wave energy systems create the appearance or artifact of neutral or insignificant trends for about 45 % of global oceans and seas. In the present study, the global wave energy climate changes are classified into six types based on the mixed trends in the wave energy systems, which reveals that more than ninety percent of the global wave sites are experiencing significant changes in wave energy systems and climates. It highlights the need for increased scrutiny of risks for coastal and ocean communities and design practices to ensure the resilience of coastal defense and other marine energy infrastructure, e.g., offshore wind and wave energy farms.

ABBREVIATIONS

WEC	Wave Energy Converter
ECMW	European Centre for Medium-Range Weather Forecasts
ERA5	fifth generation ECMWF reanalysis
WAM	Wave Model
RM3	Reference Model 3

1. Introduction

Ocean wave energy has been identified as a climate change indicator as long-term trends in wind climates and sea surface temperature are the historical drivers of wave energy climate changes (Reguero et al., 2019). As ocean wave energy contributions to the global energy portfolios continue to expand over the next few decades (Hand et al., 2012), investigating long-term trends in the global wave energy climate is vitally important for planning wave energy projects and designing wave energy converter (WEC) technologies. Such investigations are also important to inform ocean and coastal management policy and design practices to ensure the resilience of offshore infrastructure, e.g., offshore wind and wave energy farms, and coastal defenses (Hansom et al., 2014).

All studies to date investigate historical linear trends in summary bulk wave parameters, e.g., omnidirectional wave power (sum of energy within wave systems in all wave periods and directions) and mean significant wave height. Henceforth, *wave power* is used in place of omnidirectional wave power. These studies have reported multi-decade trends with increasing wave power and mean significant wave height at high latitudes of the southern hemisphere and decreasing trends in the North Pacific Ocean. Reguero et al. (2019) and Young et al. (2011) investigated linear trends of mean wave power and significant wave height from 1985 to 2008 and showed 1.0–2.0 %/year increases in the southern oceans. Reguero et al. (2015) showed that differences in the mean wave power during the 2001–2008 period with respect to the mean wave power during the 1981–1990 period in the North Pacific Ocean were negative 5.0–10.0 kW/m. Young and Ribal (2019) highlighted that the significant wave height in the North Pacific Ocean decreased by 0.5 cm/year from 1985 to 2018. Timmermans et al. (2020) intercompared global wave height trends during the 1992–2017 period

* Corresponding author.
E-mail address: sahn@jejunu.ac.kr (S. Ahn).

https://doi.org/10.1016/j.jclepro.2024.143758
Received 13 February 2024; Received in revised form 23 August 2024; Accepted 20 September 2024
Available online 21 September 2024
0959-6526/

using multi-mission satellite altimeter products and wave model hindcasts and observed consistent increasing trends at high latitudes of the southern oceans and decreasing trends in the North Pacific Ocean. Shi et al. (2024) investigated global historical trends in significant wave height of tropical cyclones using 44-year wave reanalysis and showed that maximum significant wave heights have increased by about 3%/decade globally. Zheng et al. (2022) investigated global wave height trends of wind seas and swells and highlighted regional differences and similarities between the trends of wind seas and swells. These previous investigations including recent regional studies, e.g., Canadian waters (Dong et al., 2023), Chinese waters (Sun et al., 2022), Mediterranean Sea (De Leo et al., 2024), North Indian Ocean (Kerkar and Seelam, 2024), and Arctic Ocean (Christakos et al., 2024), focused on highlighting wave sites with statistically significant trends in the bulk wave parameters. Future wave climate changes under various carbon-reduction scenarios have been widely investigated but these studies also focus on changes in the bulk wave parameters, e.g., Rusu (2019), Lemos et al. (2019), Meucci et al. (2023), Mohamad et al. (2020) and Casas-Prat et al. (2024).

Although there is a range of results depending on data sources and periods of record, all previous studies have shown that long-term historic trends in the bulk wave parameters are neutral or statistically insignificant at more than half the global wave sites. Reguero et al. (2019) showed that the linear trends in wave power in the North Atlantic and Indian Oceans range from negative trends of - 0.5 %/year to positive trends of +0.5 %/year that are statistically insignificant at the 95% confidence level. The mean significant wave height trends estimated by Young et al. (2011) and Timmermans et al. (2020) are not statistically significant at most global wave sites except for the North Pacific Ocean and the high-latitude regions of the southern oceans. Young and Ribal (2019) revealed that the linear trends in significant wave height in the equatorial waters are neutral. While a quantitative comparison of the results from previous studies is not appropriate given differences in data sources, methodologies, and periods of record (Timmermans et al., 2020), most studies commonly showed that the trends in the bulk wave parameters are neutral or statistically insignificant at more than half the global wave sites. As a result, wave energy climate changes in these regions have received less attention and the future risks for these coastal and ocean communities are not appreciated. Are wave energy climate trends in these regions not affected by global climate change or are existing wave energy climate metrics and methodologies not of adequate fidelity to detect trends?

Ocean waves are formed by the superposition of individual waves having different frequencies and directions, called wave systems. As the wave power at a particular location is a sum of the energy constituents of multiple wave energy systems (Goda, 2010), which are generated by remote and local wind systems (Echevarria et al., 2019), these wave energy systems exhibit different long-term trends driven by changes occurring for distinct wind climate systems (Ahn and Neary, 2020). Addressing these questions and investigating trends in different wave energy systems are crucial for the coastal and ocean infrastructure projects including offshore wind and wave energy farms that simplify the wave energy climate changes based on the bulk wave parameter trends. For wave energy projects, wave energy absorptions are generally constrained to a narrow wave period band (Ghasemipour et al., 2022) as common types of wave energy converters maximize the energy production by resonating at a similar period of energetic waves (Dallman and Neary, 2014). For example for bi-modal wave climates exhibiting two distinct wave energy systems within different period bands, e.g., Hawaii in the United States (Ahn et al., 2020), wave energy projects with common wave energy converters operating within a narrow period band (Zhou et al., 2023) need to identify a dominant wave energy system and investigate its long-term trend rather than the trend of total wave power. For small-scale wave projects targeting short-period wave systems, e.g., marine observations and microgrids, trends in short-period wave systems and long-period wave systems need to be separately investigated for planning future energy productions and assessing design loads.

However, the previous approach only investigates trends in the bulk wave parameters that lumps trends of the individual wave systems and classifies trends as either positive, negative or neutral. The present study introduces a new approach for identifying and characterizing mixed trends in the wave energy systems using a 42-year global wave reanalysis. The historical long-term trends in global wave energy systems are investigated by resolving trends of period-resolved and period-directionally resolved wave energy, in which wave energy is partitioned into discrete wave periods and directions, rather than resolving trends of the wave power (total wave energy in all periods and directions). Assessing the period and directionally resolved wave energy enables discernment of trends in individual wave energy systems (Hanson and Phillips, 2001) and links their trends with those in the wind climates (Ahn and Neary, 2021). The new approach detailed herein resolves the trend for each wave system and can determine whether the trend based on bulk parameters is an artifact of lumping trends of individual wave systems. The global wave energy climate changes are delineated into six trend classes based on combinations of the mixed trends, e.g. mixed but positive trend or weighted or positive trend dominated. This new approach reveals the startling result that nonstationary historical trends have in fact been more pervasive around the globe than results in previous studies have shown.

Herein, a new high-fidelity frequency and directionally resolving approach is introduced to investigate nonstationary trends in wave energy climate through individual wave systems rather than single bulk wave parameters. The present investigation includes three focus areas: 1) Characterization of linear trends in period-resolved wave energy systems, 2) Delineation of global oceans and seas based on the degree of mixed trends in distinct wave energy systems, and 3) Elucidation of underlying mechanisms of the mixed trends by linking period-directionally resolved wave energy trends and commensurate trends in the wind climate.

2. Methodology

Our methodology for investigating trends in the wave energy systems is summarized in Fig. 1. This methodology is applied to a 0.5° spatial resolution of global wave reanalysis spanning forty-two years (1979–2020) created by the fifth generation ECMWF (European Centre for Medium-Range Weather Forecasts) reanalysis (ERA5) (Hersbach et al., 2020). Using spectral partitioned wave parameters of ERA5, joint distributions of annual wave energy in terms of wave periods and directions are computed to resolve wave energy contents within each wave period and direction bin. The long-term linear trends of the 42-year annual joint wave energy distributions are computed using the Least-squares linear regression and the statistical significances of the trends are determined using the Mann-Kendall significance test (Kendall, 1984). The global wave sites are delineated based on the inter-annual linear trends of the joint wave energy distribution to identify wave sites exhibiting mixed trends. Finally, underlying mechanisms of the mixed trends are illustrated by linking period and directionally resolved wave energy trends and commensurate trends in the wind climate.

2.1. Data source

As periods of record of wave measurement data are not sufficient to assess the long-term trends, the investigations of wave energy trends need to rely on the long-term wave hindcast simulation data, which are assimilated with and validated to the wave measurements. While long-term frequency-directional (2D) wave spectra of the model hindcast over the global domain would provide a higher fidelity assessment, they are not currently available because the large size of these datasets makes storage impractical. Spectral partitioned wave parameters are the only available data source for investigating the long-term trends in global

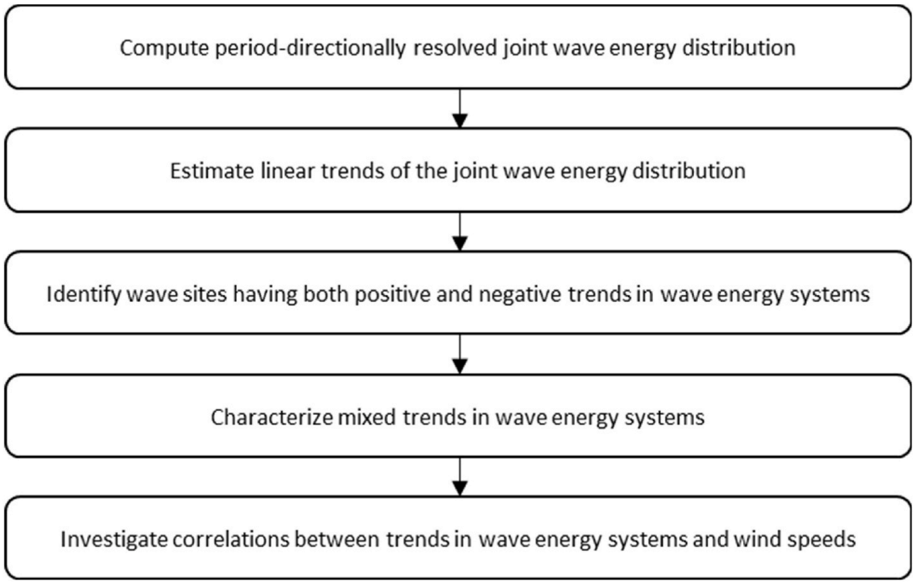

Fig. 1. Flow chart of the methodology with steps adopted for investigating mixed trends in wave energy systems.

wave energy systems.

ERA5 provides hourly partitioned wave parameters from 1950 onwards generated from a fully-coupled atmosphere-wave model (WAM) with assimilations of altimeter-derived wave height data. ERA5 decomposes the modeled frequency-directional wave spectrum into multiple partitions representing the energy of independent wave systems within the spectrum using a watershed identification algorithm (Hanson and Phillips, 2001) and provides spectral partitioned wave parameters of each wave system. Detailed information on the spectral partitioning process adopted in ERA5 can be found in the following reference (Bidlot, 2020). The significant wave height, energy period, and mean wave direction of partitioned wave systems, spectral partitioned wave parameters, are used rather than those of the entire wave spectrum, bulk wave parameters, to better resolve long-term trends in distinct wave systems. The bulk wave parameters cannot resolve multi-model wave climates as they are mean (or peak) statistics of combined wave energy systems.

The partitioned wave parameters have provided advantages over the bulk parameters in wave climate investigations including wave modeling (Kumar et al., 2017), multimodal wave climate characterizations (Romano-Moreno et al., 2023), wave energy resource assessments and characterizations (Yang et al., 2023), regional (Ahn et al., 2019) and global (Ahn et al., 2022) wave energy resource classifications. The wave data prior to 1979 is not considered as ERA5 assimilates winds and wave heights throughout the periods from 1979 to 1991 onwards and it is commonly recommended to independently investigate long-term trends for the periods before and after 1979 (Reguero et al., 2015).

The ERA5 reanalysis has been extensively validated to in-situ measurement and altimeter data. The ERA5 significant wave heights were validated against measurements from 103 National Data Buoy Centre buoys in the North Pacific and Atlantic coasts over the 1979–2019 period (Wang and Wang, 2022) and reported that the accuracy of the modeled significant wave height is satisfactory under typical sea states (<4 m) with 0.961 correlation coefficient, −0.058 bias, and 18.54% scatter index on average. The bias in wave power estimates derived from the ERA5 reanalysis ranges from - 10 to +15 % at most global wave sites (Rusu and Rusu, 2021) which specifies the maximum acceptable bias error, 25 % (for a reconnaissance wave resource assessment), defined by the International Electrotechnical Commission standard: TS 62600–101 (IEC, 2015).

NOAA's WaveWatch3 hindcast (National Oceanic and Atmospheric Administration, 2020) is an alternative data source that provides the global spectral partitioned wave parameters. This data is not considered herein as it has a relatively short period of record of 31-year (1979–2009) compared to the ERA5. The present study assumes the uncertainties and sensitivities from different data sources are negligible for estimating annual mean statistics and inter-annual linear trends as both ERA5 and NOAA's WaveWatch3 hindcasts have been extensively validated to in-situ measurement and assimilated with altimeter data.

2.2. Energy of partitioned wave systems

The wave power transmitted by each partitioned wave system, J_P (kW/m), is computed as

$$J_P = \frac{\rho g}{16} {Hs_P}^2 Cg_P \tag{1}$$

where ρ is the water density (1025 kg/m^3), Hs_P (m) is the significant wave height of a partitioned wave system and Cg_P (m/s) is the group velocity of the partitioned wave system defined as

$$Cg_P = \frac{2\pi}{k_P}\left(1 + \frac{2k_P h}{\sin h(2k_P h)}\right)\frac{1}{Te_P} \tag{2}$$

The wave number, k_P (m^{-1}), and energy period, Te_P (s), of the partitioned wave system and depth, h (m), are related through the dispersion equation as

$$\left(\frac{2\pi}{Te_P}\right)^2 = gk_P \tan h\,(kh) \tag{3}$$

The significant wave height (Hs_P) and energy period (Te_P) of a partitioned wave spectrum are computed as $4\sqrt{m_0}$ and m_{-1}/m_0, respectively, where the parameter m_n is the nth-order spectral moment.

To resolve energy distributions of wave systems over the wave periods and directions and quantify their inter-annual linear trends, the energy of all individual partitioned wave systems, J_P, are sorted into three-dimensional bins resolving periods (T_b, thirty-bins from 0 to 30 s with a resolution of 1 s, e.g., $T_b = 1$ means 0 s $< T \leq 1$ s), directions (θ_b, thirty-six bins with a resolution of 10° clockwise from true North, e.g., $\theta_b = 1$ means $0^\circ < \theta \leq 10^\circ$), and inter-annual (Y, forty-two years from 1979 to 2020) based on their energy period (Te), mean direction (θ), and year (y). The inter-annual mean energy of resolved wave systems, $J(T_b, \theta_b, Y)$ (kW/m), is computed as the summation of J_P within each cell in the 3-D matrix (T_b, θ_b, Y) divided by the number of data hours, N, in the corresponding year as

$$J(T_b, \theta_b, Y) = \sum J_{P(T \in T_b, \theta \in \theta_b, y=Y)} \Big/ N \tag{4}$$

This method of computing the period-directionally resolved wave energy distribution was validated to various data sources including in-situ buoy measurements (Ahn et al., 2023), Global Wave Watch III hindcast (Ahn et al., 2022), and regional wave hindcast (Ahn et al., 2021). The inter-annual mean wave energy in terms of wave period, $J(T_b, Y)$, is taken as the summation over the direction bins and the inter-annual mean wave power (sum of wave energy in all periods and directions), $J(Y)$, is computed as the summation of all wave energy constituents in the entire period and direction bins. The 42-year mean wave power, J, is simply the mean value of $J(Y)$. Herein, a wave energy system is defined as the mean wave energy constituents within each period and directional bin.

2.3. Inter-annual linear trends of wave energy systems

The inter-annual mean values of wind speeds, $W(Y)$, wave power, $J(Y)$, period-resolved wave energy, $J(T_b,\ Y)$, period-directionally resolved wave energy, $J(T_b, \theta_b, Y)$, and energy period, $Te(Y)$, spanning 42 years are computed to examine linear trends in wave energy systems. The wave climates exhibit nonstationarity at various time scales, e.g., seasonal, interannual, and interdecadal. The present study investigates long-term linear trends over 42 years by adopting a general definition of "nonstationary" that climate systems change over time (J. Méndez and Rueda, 2020). The long-term trends of these variables are estimated using the Least-squares linear regression. For example, the average rate change of inter-annual mean wave power within $T_b = 1$, $J(1, Y)$, is given by the slope, A, in the linear equation $J(1, Y) = AY + B$, which represents the best fit linear trendline in a least-squares sense. The statistical significance of the trends is determined using the Mann-Kendall significance test (Kendall, 1984). The Mann-Kendall test determines whether or not a trend is a monotonic upward or downward over time and whether the trend in either direction is statistically significant (Young et al., 2011). The Least-squares linear regression and Mann-Kendall test are adopted in the present study as these are the common types of analysis in the earth sciences especially in wind and wave climate trend studies (Reguero et al., 2019). A previous study intercomparing various methods showed that other statistical approaches, e.g., the Seasonal Kendall test (Hirsch et al., 1982) and Singular Spectrum Analysis (Alexandrov et al., 2008), produced similar results to the present method in estimating linear trends of bulk wave parameters (Young et al., 2011). The present study assumes that variations in estimating trends in the wave energy systems from the common statistical methods are insignificant.

Fig. 2 illustrates linear trends (grey bars) of inter-annual mean wave energy constituents within each period bin, $J(T_b, Y)$, at a sample site.

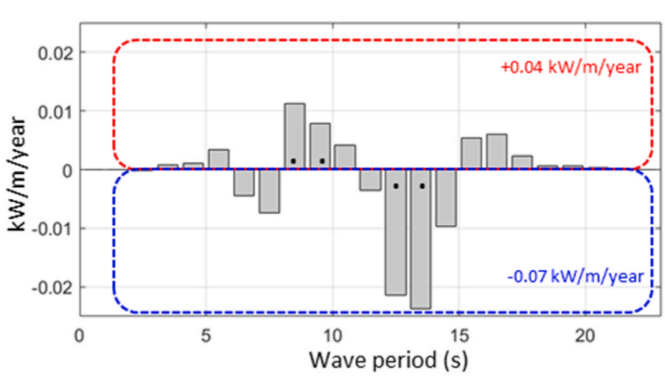

Fig. 2. Linear trends of 42-year inter-annual mean wave energy constituents in terms of the wave period bins in kW/m/year (grey bars) at a sample location (0 ° N, 130 ° W). The dots mark trends that are significant at a 95 % confidence level according to the Mann–Kendall test.

This example shows that the wave energy systems within 8–10 s wave periods have a positive trend (+0.02 kW/m/year) while the wave energy systems within 12–14s wave periods have a negative trend (−0.04 kW/m/year).

2.4. Identifying mixed trends in wave energy systems

The inter-annual linear trends of wave energy systems at the sample location (0 ° N, 130 ° W) shown in Fig. 2 illustrate the mixed opposing trends in the wave energy systems. To identify global wave sites exhibiting mixed trends, the degree of the mixed trends is quantified based on the following procedure. The wave period bins at each wave site are separated into two groups based on the sign of trends in the corresponding period-resolved wave energy. The positive trend at each wave site is computed as the sum of the linear trends within positive period bins relative to their 42-year mean value (+0.04 kW/m/year in Fig. 2). The negative trend at each wave site is computed as the sum of the linear trends within negative period bins relative to their 42-year mean value (−0.07 kW/m/year in Fig. 2). Wave sites exhibiting both positive and negative trends are identified based on relative ranges between the positive and negative trends. The period-resolve wave energy trends, regression slopes of $J(T_b, Y)$, in these wave sites are investigated to characterize mixed trends in the wave energy systems.

3. Results

The linear trend of the wave power (sum of wave energy in all periods and directions) is presented in Section 3.1. In Section 3.2, linear trends of period-resolved wave energy systems and mixed trends are described and global wave sites are classified into six types based on the mixed trends in the wave energy systems. In Section 3.3, global wave sites exhibiting significant mixed trends in the wave energy systems are identified and underlying mechanisms of the mixed trends at representative wave sites are discussed by linking period-directionally resolved wave energy trends and commensurate trends in the global wind speed.

3.1. Global wave power trends

The geographic distribution of the 42-year mean wave power (sum of wave energy in all periods and directions) is shown in Fig. 3 (a). The high-latitude oceans at 30 - 60 ° in both Hemispheres exhibit larger wave power than the low-latitude oceans as the westerlies are stronger than the trade winds (Cornett, 2008). In the high-latitude regions, the southern hemisphere oceans have more wave power with longer fetch than the northern hemisphere. The spatial pattern of linear trends in the inter-annual mean wave power shown in Fig. 3 (b) is like those of the previous studies summarized in Section 1. The wave power over the globe has predominantly increased, while the trends in many oceans, including the eastern equatorial Pacific Ocean and temperate zones in the North Pacific, North Atlantic, and Indian Ocean (dots in Fig. 3 (b)) are neutral or statistically insignificant.

3.2. Trends in period-resolved wave energy systems

These observed trends in bulk wave parameters, viz., wave power and significant wave height, whether nonstationary or stationary, may not reflect those occurring for wave energy climates because they integrate all wave systems in the directionally and frequency-resolved wave spectrum. Regional wave climates are, in fact, determined by multiple wave energy systems that experience different long-term trends. For example at a wave site located in the eastern equatorial Pacific Ocean (0 ° N, 130 ° W), while the linear trend of the wave power is neutral, i.e., close to zero (Fig. 3 (b)), trends in different wave energy systems in terms of the wave period shown in Fig. 4 (a) reveal that dominant wave energy systems containing the large energy, e.g., wave systems in 8–11 s and 11–15 s, have opposite historical long-term trends and offset each

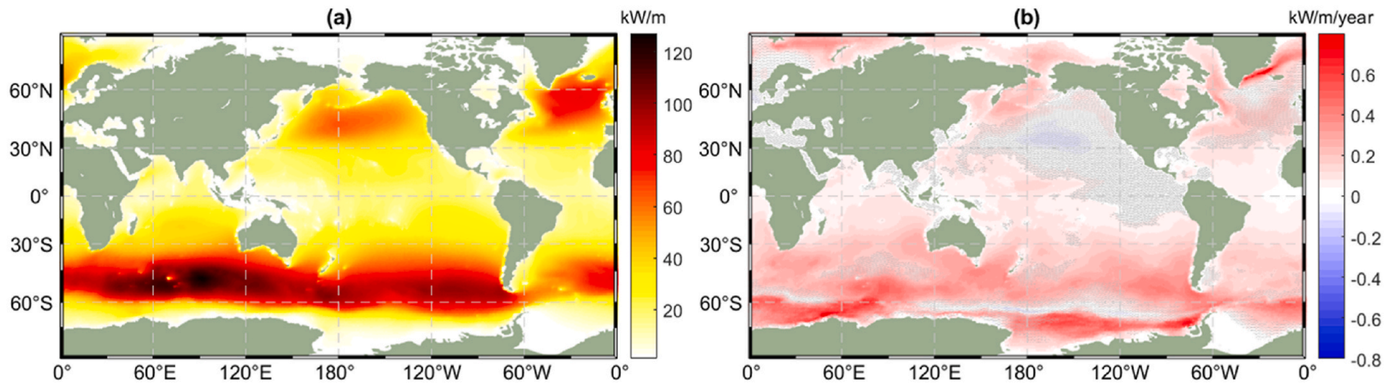

Fig. 3. (a) 42-year mean wave power in kW/m. (b) Linear trends of inter-annual mean wave power in kW/m/year. The dots mark trends that are not significant at a 95 % confidence level according to the Mann–Kendall test (Kendall, 1984).

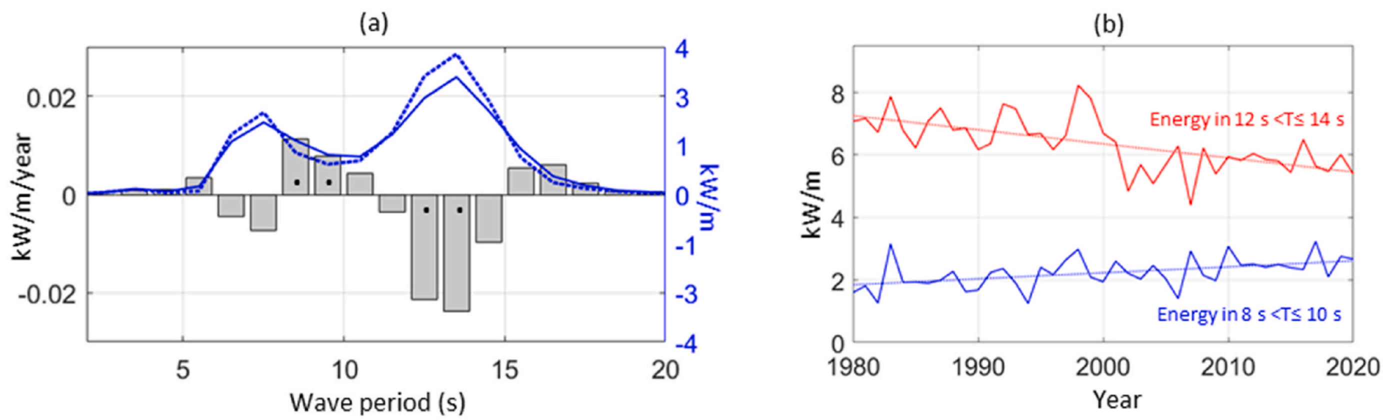

Fig. 4. (a) Linear trends of 42-year inter-annual mean wave energy constituents in terms of the wave period bins in kW/m/year (grey bars in left-axis), and 20-year mean wave energy constituents in kW/m (blue dash line: 1981–2000, blue solid line: 2001–2020) at a sample location (0 ° N, 130 ° W). The dots mark trends that are significant at a 95 % confidence level according to the Mann–Kendall test. (b) Inter-annual mean wave energy within 8 s–10 s (blue) and 12 s–14 s (red) and corresponding linear trends (dash lines) at the same location. (For interpretation of the references to color in this figure legend, the reader is referred to the Web version of this article.)

other, neutralizing trends in integrated bulk wave parameters. The two linear trendlines of inter-annual mean wave energy within 8–10 s and 12–14 s, which are statistically significant show the average rate of positive (+0.8 %/year) and negative (-0.7 %/year) changes over the 42 years. Assuming these opposing trends continue in the future, the bimodal wave energy climate at this site can turn into an unimodal one, in which the most dominant wave energy system can be changed and the seasonal energy variation can be reduced, significantly influencing marine energy projects, coastal resiliency planning, and future risks. Therefore, understanding trends in wave energy systems beyond simple integrated bulk wave parameters is vitally important.

Fig. 4 illustrates that both positive (increasing) and negative (decreasing) trends of wave energy systems in different wave periods occur at the same wave site. To characterize and quantify the mixed trend, wave period bins at each wave site are separated into two groups based on the sign of the corresponding period-resolved energy trends. The positive trend at each wave site is computed as a linear trend of inter-annual mean wave energy within positive period bins relative to their 42-year mean value (Fig. 5 (a)). The negative trend at each wave site is computed as a linear trend of inter-annual mean wave energy within negative period bins relative to their 42-year mean value (Fig. 5 (b)).

Fig. 5 (a) indicates that 75 %, 36 %, and 8 % of global wave sites have wave energy systems with positive trends over 0.3 %/year, 0.5 %/year, and 2.0 %/year, respectively. The changes that are not statistically significant at a 95 % confidence level according to the Mann–Kendall test are marked with the white color. The largest increases of over 2.0 %/year relative to the mean wave power are mainly observed along the high-latitude regions where the mean wave power is small. In the northern hemisphere Pacific, Atlantic, and Indian Oceans, the western side oceans tend to have larger relative increases compared to the eastern side oceans given historical positive trends in trade winds (Young and Ribal, 2019). The 15 % wave sites have no positive wave energy systems, e.g., the North Pacific Ocean, which are marked with the white color in (Fig. 5 (a)).

The negative trends are observed over half the global wave sites where the largest energy decrease relative to the mean wave power is found in the eastern equatorial Pacific Ocean over - 0.3 %/year (Fig. 5 (b)). The high-latitude regions near the Arctic and Antarctic have no negative wave energy systems. The - 0.05 %/year threshold is the 99.0 percentile of negative trends in Fig. 5 (b) and +0.05 %/year is applied as a lower bound of positive trends in Fig. 5 (a). The upper bounds, +9.0 %/year and −0.5 %/year, are the 99.0 percentile of positive trends and 1.0 percentile of negative trends.

In Fig. 6, the global wave energy climate changes are classified into six types based on the ranges of separated trends in positive and negative wave energy systems delineated in Fig. 5: Type 1 (magenta, 41 %) - dominated by positive trends (statistically significant positive trend wave energy systems over 0.05 %/year without negative trend wave energy systems), Type 2 (black, 37 %) - mixed but weighted to positive trends (range of positive trend wave energy systems > range of negative trend wave energy systems), Type 3 (orange, 6 %) - mixed and neutral

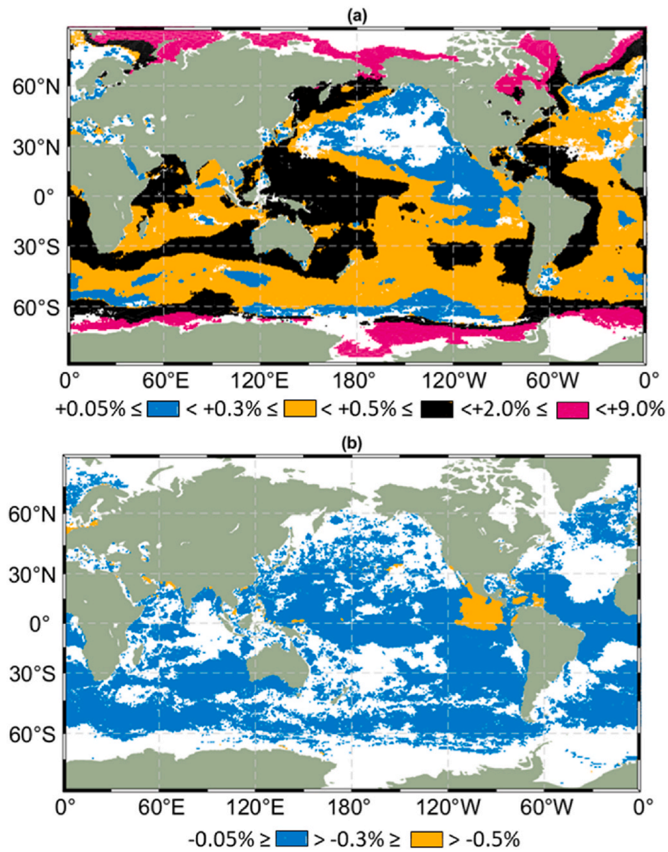

Fig. 5. Separated trends of (a) positive wave energy systems and (b) negative wave energy systems relative to 42-year mean wave power in %/year. Colors indicate ranges of the percent changes. (For interpretation of the references to color in this figure legend, the reader is referred to the Web version of this article.)

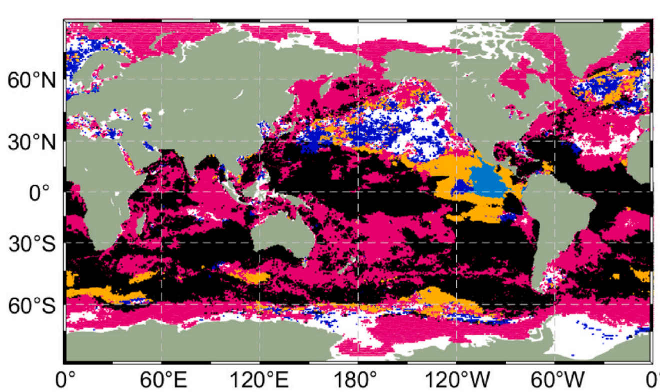

Fig. 6. Six types of global wave energy climate changes: Type 1 (magenta) - dominated by positive trends, Type 2 (black) - mixed but weighted to positive trends, Type 3 (orange) - mixed and neutral trends, Type 4 (sky-blue) - mixed but weighted to negative trends, Type 5 (blue) - dominated by negative trends, Type 6 (white) - neutral trends. Detailed descriptions are provided in Table 1. (For interpretation of the references to color in this figure legend, the reader is referred to the Web version of this article.)

trends (range of positive trend wave energy systems = range of negative trend wave energy systems), Type 4 (sky-blue, 2 %) - mixed but weighted to negative trends (range of positive trend wave energy systems < range of negative trend wave energy systems), Type 5 (blue, 5 %) - dominated by negative trends (statistically significant negative trend wave energy systems over - 0.05 %/year without positive trend wave energy systems), Type 6 (white, 9 %) - neutral trends (neutral or statistically insignificant in both positive and negative trend wave energy systems). Predominantly positive wave energy trends (Type 1, magenta) are observed along the western border of the southern Pacific and southern Atlantic Oceans, North Atlantic temperate zone, and eastern Indian Ocean. The wave climates in these regions are unimodal, i.e., dominated by a single wave system, where increasing prevailing wind systems drive the positive wave energy trends. The wave system in the middle of the northern Pacific Ocean is generated by Pacific westerlies where the wave energy trends are dominated by the negative trends (Type 5, blue) due to the southward migration of the jet stream (Vitousek et al., 2009). Only 9 % of global wave sites mainly located in the northeast Pacific Ocean have neutral trends (Type 6, white) where both positive and negative wave energy trends are statistically insignificant. The 50 % wave sites have mixed trends in positive and negative wave energy systems (Types 2–4). The trends in the eastern sides of the southern Pacific, Atlantic, and Indian Oceans and western sides of the equatorial Pacific and Atlantic Oceans are weighted to the positive trends (Type 2, black). The eastern equatorial Pacific Ocean has unique mixed trends, which are weighed to the negative trends (Type 4, sky-blue). The positive and negative wave energy trends offset each other at the wave sites (Type 3, orange) in the eastern equatorial Pacific Ocean, eastern North Atlantic temperate zone, and pockets in the high-latitude southern oceans.

3.3. Mixed trends in global wave energy systems

In Fig. 7, the top-left map highlights regions exhibiting mixed trends by quantifying relative ratios of negative trends to the absolute sum of positive and negative trends. A relative ratio of one means all wave energy systems have negative trends while 0.5 means positive and negative trends of wave energy systems are equal and neutralize the wave power trend. In the central North Pacific Ocean and North Sea (east sea of United Kingdom) more than 80 % of trends in wave energy systems are negative. In the eastern equatorial Pacific Ocean and northern Atlantic Ocean temperate zone, about 50–70 % of wave energy trends are negative, which implies that 30–50 % of trends in different wave period bands are positive during the same period of record. As shown in Fig. 6, mixed trends are also observed in the Indian Ocean temperate zone and South Pacific Ocean subtropics where 20–40 % of trends in the wave energy systems are negative.

The majority of global wave sites known to have no significant wave power trends (marked with dots in Fig. 3 (b)) are located in the regions having both positive and negative trends in wave energy systems with moderate to high ratio values in Fig. 7. In contrast to the previous studies, the present study reveals that these regions also have experienced significant wave energy climate changes, which are even more dynamic than regions dominated by either positive or negative trends. Fig. 7(a–f) illustrates trends of wave energy systems at wave sites located in these highlighted regions. Except for the wave site (a) located in the North Pacific, these wave sites represent the mixed wave energy trends: (b) mixed and neutral trends (c) mixed but weighted to negative trends (d, e, f) mixed but weighted to positive trends.

The high-latitude sites in both hemispheres (a, b, e, f) have an unimodal wave energy distribution centered in the 10–12 s period band. The wave energy systems within shorter and longer period bands relative to this peak period have experienced opposite historical trends at these sites except for (a). The longer period waves (11–15 s) have increased while the shorter period waves (<11 s) have decreased (Fig. 7 (b–e, f)), resulting in the energy shift towards the long period band. The normal distribution shapes of wave energy in 1981–2000 (dash-line) changed to negatively skewed distributions in 2001–2020 (solid-line) at these sites. More dynamic changes are observed in some of the equatorial oceans currently known to have neutral wave power trends. Unlike the high-latitude oceans, the equatorial oceans have bimodal wave energy distributions, centered in 7–8 s and 12–14 s period bands (Fig. 7

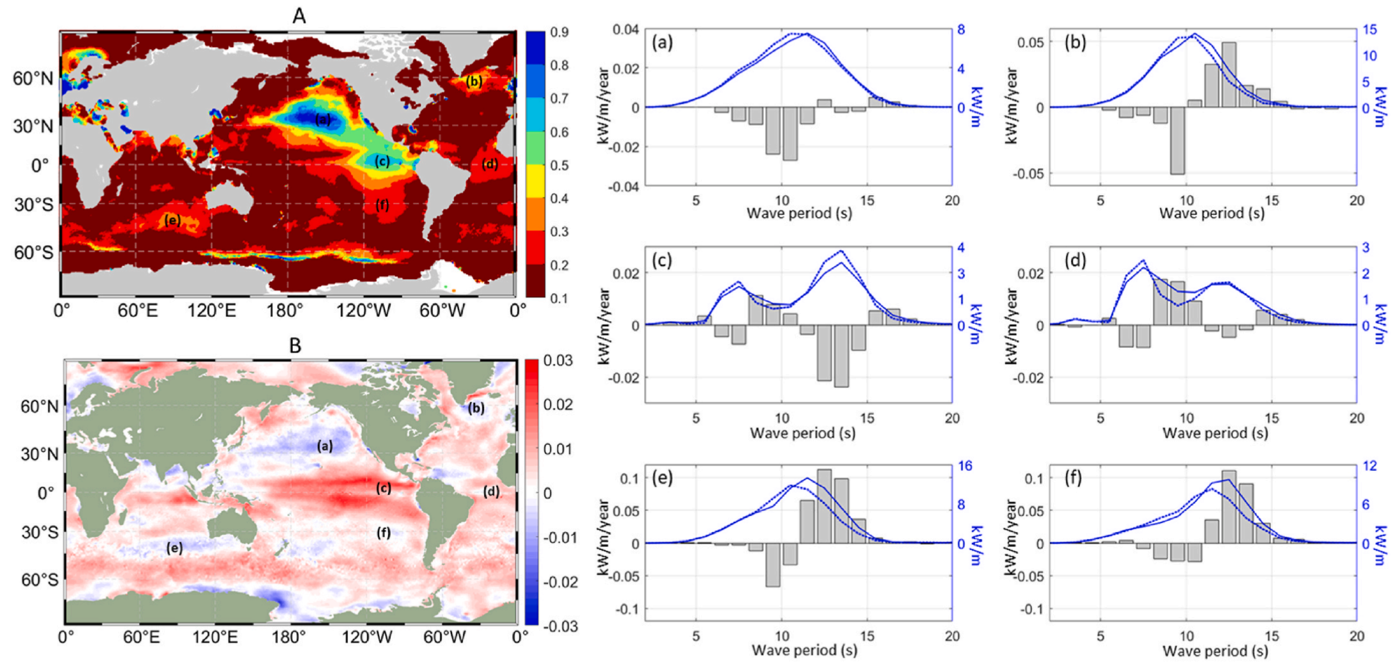

Fig. 7. A. The ratio of trends in negative wave energy systems to trends of all wave energy systems (absolute sum of negative bars/sum of absolute values of all bars in subfigures). B. Linear trends of inter-annual mean wind speed in m/s/year. (a–f) Linear trends of wave energy systems in terms of wave periods (grey bars in left-axis) and 20-year mean wave energy systems (blue dash line: 1981–2000, blue solid line: 2001–2020) at sites of regional sub-peaks in the ratio map. (For interpretation of the references to color in this figure legend, the reader is referred to the Web version of this article.)

Table 1
Six types of global wave energy climate changes.

Type		Description
1	Dominated by positive trends	Statistically significant positive trend wave energy systems over 0.05 %/year without negative trend wave energy systems
2	Mixed but weighted to positive trends	Range of positive trend wave energy systems > range of negative trend wave energy systems
3	Mixed and neutral trends	Range of positive trend wave energy systems = range of negative trend wave energy systems
4	Mixed but weighted to negative trends	Range of positive trend wave energy systems < range of negative trend wave energy systems
5	Dominated by negative trends	Statistically significant negative trend wave energy systems over – 0.05 %/year without positive trend wave energy systems
6	Neutral trends	Neutral or statistically insignificant in both positive and negative trend wave energy systems

(c and d)). The peakedness of the bimodal energy distributions has been reduced as wave energy systems within both peak period bands have decreased while the wave energy systems within 8–11s have increased in these equatorial oceans.

As described in previous research (Reguero et al., 2019), intensified wind speed as a consequence of global warming is the primary driver of observed positive wave energy trends. While wind speeds over global wave sites have predominantly increased, some regions have experienced negative wind speed trends (Reguero et al., 2019). The weakened westerlies over a wide region of the central north Pacific Ocean reduced the energy of overall wave energy systems passing through this region (Fig. 7 (a)). The wave sites exhibiting mixed trends in the wave energy systems mainly lay in regions where the local wind speeds have decreased during the same period of record (Fig. 7 bottom-left). At four representative wave sites exhibiting mixed wave energy trends (Fig. 7 (b–d, e, f)), weakened local wind speeds reduced the energy within short-period wave energy systems. Fig. 8 describes linear trends of the inter-annual mean period-directionally resolved (2D) wave energy systems at wave sites, (b) and (e) in Fig. 7, representing these trends in wave energy systems. Fig. 8 (a) shows that the negative trends in short-period wave energy systems at the North Atlantic wave site are mainly due to weakened local westerlies. Two different long-period wave systems that pass through this wave site come from the northeast and southwest directions and have positive trends. Unlike the North Atlantic wave site, the wave energy systems and their trends are directionally focused at the Indian wave site as shown in Fig. 8 (b). In this wave site, the intensified westerlies in the southern Atlantic Ocean increase the long-period wave energy systems while the weakened local wind speed results in the negative trends of the short-period wave systems.

Trends in directionally resolved (1D) wave energy are not discussed in the present study because they mix different and distinct trends in ocean wave systems, which are conventionally classified based on their frequencies. The directionally resolved wave energy trends would mask the negative and positive trends in distinct wave energy systems at the North Atlantic and Indian wave sites shown in Fig. 8.

The largest increases in the mean wind speed exceeding 0.02 m/s/year are observed in the eastern equatorial Pacific Ocean (Fig. 7 bottom-left). It is the result of intensified trade winds associated with the sea-surface temperature increase near the Equator (Timmermann et al., 2010) and the equatorward-shifted Pacific High-pressure system (Vitousek et al., 2009). Despite the strengthening of the local trade winds and resultant positive short-period (8–11 s) wave energy systems, this region has experienced neutral wave power trends (Fig. 3 (b)) due to decreasing long-period (11–15 s) wave energy systems (Fig. 7 (c)). A primary driver of the observed negative trends in the long-period wave energy systems needs to be determined to characterize and predict the regional wave energy climate changes.

To elucidate the underlying mechanism of the mixed trend at the wave site (c) located in the eastern equatorial Pacific Ocean, linear trends of the inter-annual mean period-directionally resolved wave energy systems are described in Fig. 9 (a). It reveals that the long-period wave energy systems with the negative trend at this site mainly originate from the northeast direction. This negative trend of wave energy

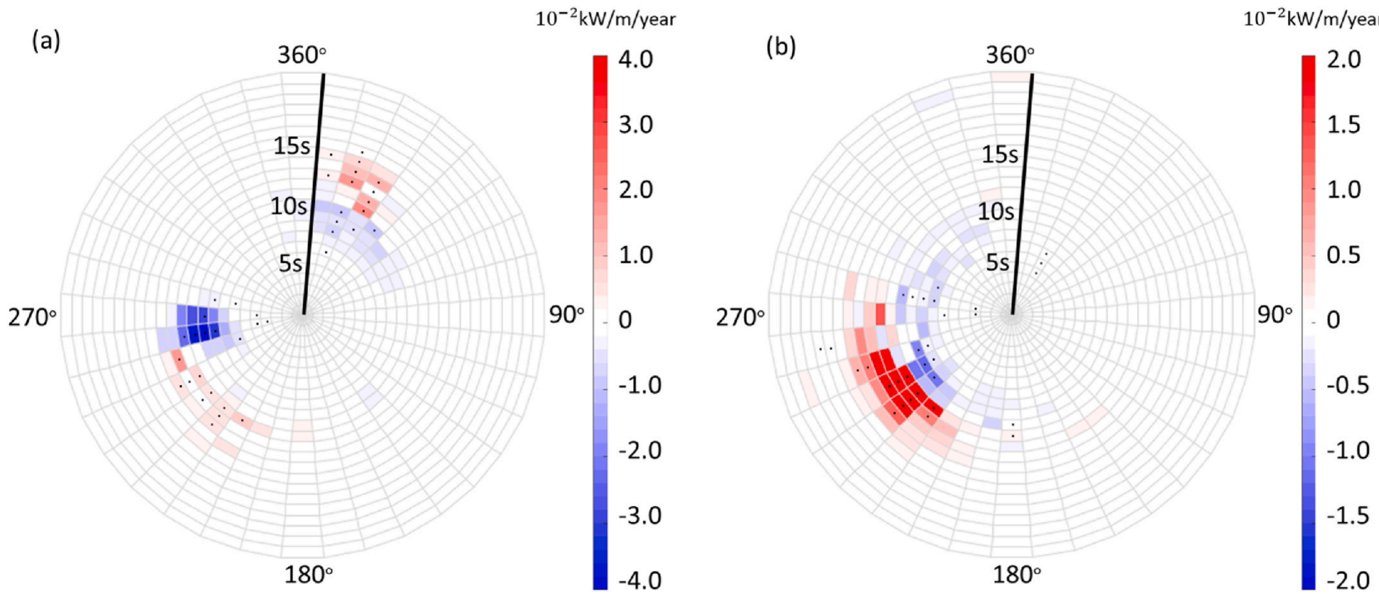

Fig. 8. Linear trends of 42-year mean wave energy systems in terms of periods and directions: (a) North Atlantic wave site ((b) in Fig. 7), (b) Indian Ocean wave site ((e) in Fig. 7). The dots mark trends that are statistically significant at a 95 % confidence level according to the Mann–Kendall test.

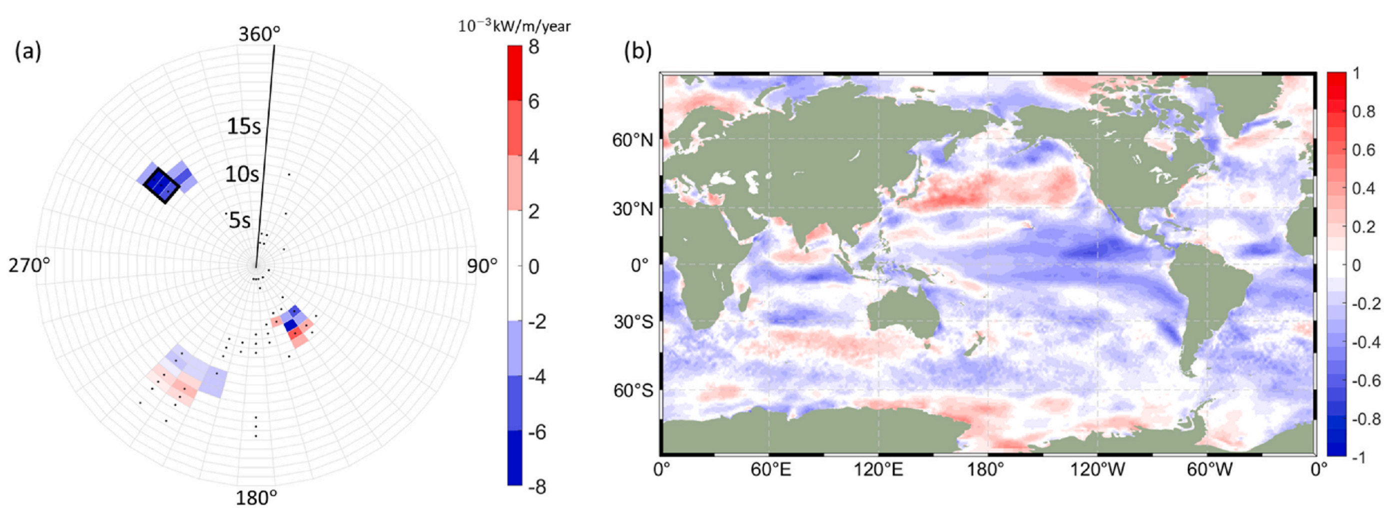

Fig. 9. (a) Linear trends of 42-year mean wave energy systems in terms of periods and directions at the sample site (0 ° N, 130 ° W). The dots mark trends that are statistically significant at a 95 % confidence level according to the Mann–Kendall test. (b) Geographic distribution of Pearson correlation coefficients between inter-annual mean wind speed at global wave sites and inter-annual mean wave energy system within 305–315 ° within 12–15 s (black box in Fig. 9 (a)) at the sample site. The colors are correlations that are statistically significant at a 95 % confidence level of the Student's t-test. (For interpretation of the references to color in this figure legend, the reader is referred to the Web version of this article.)

systems from 305 to 315 ° within 12–15 s (marked in a black box in Fig. 9 (a)) is statistically significant and highly correlated with negative trends in the western North Pacific westerlies (Fig. 9 (b)). In addition, intensified and southward-shifted Pacific jet streams within the North Pacific (Vitousek et al., 2009) decrease the long-period waves that reach the eastern equatorial Pacific Ocean (Reguero et al., 2015). Therefore, the intensified short-period trade wind waves (increasing trend) from the southeast counter the weakened long-period Pacific westerly waves from the northwest (decreasing trend), neutralizing the wave power trend at this site.

4. Discussions

The present study observes mixed wave energy trends and highlights the need for investigating long-term trends of individual wave energy systems rather than through bulk wave parameters that lump the wave characteristics of these systems. The mixed wave energy trends are mainly observed in the North Atlantic, eastern equatorial Pacific, and southern Indian Oceans where the wave climates consist of multi-wave systems. These mixed trends change the shapes of the spectral wave energy distribution and would result in significant changes in the wave climates if these trends continue in the future.

The study findings, while limited to changes in average wave conditions and not including other extreme effects like tropical cyclones, have significant implications for ocean and coastal planning, management strategies, design standards, and policies. Clearly, planning, management strategies, and design standards need to recognize that the wave climate has in fact been nonstationary for many decades and will likely continue into the future. As a result, relevant policies will have to adapt to a changing wave climate. The rate at which they will have to be reviewed and the degree to which they will have to be revised and adapted depends on whether the wave energy climate is intensifying (positive trend) or weakening (negative trend) and the rate that these changes have occurred historically and are anticipated to continue and perhaps intensify depending on a variety of different climate change scenarios.

Near-term wave energy projects should reflect the historical changes in the shapes of wave energy distributions on the design of conversion technologies as common archetypes of wave energy conversion technologies ideally need to resonate at the period of the dominant wave system to optimize the energy absorption and maximize the energy production (Aderinto and Li, 2019). For example, at the Atlantic Marine Energy Test Site on the west coast of Ireland (northeast Atlantic Ocean), the most frequently occurring sea state in the 1990s, with a significant wave height of 1.75m and a peak period of 8.25s, was changed to 1.75m with 8.75s. A Reference Model 3 (RM3) point absorber at this site would generate 123.1 kW in the nineties and 140.4 kW in the current wave climate (Prendergast et al., 2020) where a 0.5 s increase in the energy period (+0.0125 s/year) results in a 14 % increase in the energy production. At the Pioneer Array site within the southern Mid-Atlantic Bight along the East Coast of the United States, the most frequently occurring sea state changed from (1.25 m, 6.5 s) to (1.25 m, 7.25 s) over the past 40 years in which the 0.75 s increase in the energy period results in the 24 % increase in the energy production of the RM3 device. It can also result in major changes in techno-economic analysis and feasibility studies of potential wave projects by suggesting reconsiderations of target wave energy systems, size of technologies, capital expenditure, and levelized cost of electricity (Chang et al., 2018). Results of this study could inform the implementation of coastal defense infrastructure and upgrades, protection and enhancement of natural defenses (e.g., coastal wetlands, mangroves, and coral reefs), stricter zoning and building codes along coastlines adjacent to regions dominated by positive trends, e.g., the western border of the southern Pacific and southern Atlantic Oceans, North Atlantic temperate zone, and eastern Indian Ocean.

In addition, the waves with longer energy periods transfer more energy and have more influence on ocean and coastal communities than shorter-period waves. In deep oceans, long-period waves travel faster than short-period ones with faster energy transmission speeds (Dean and Dalrymple, 1991). As the wave approaches the coast in shallow water, the energy transmission speed of long-period waves slows down more abruptly because the energy transmission speed is only the function of water depth in shallow water. To comply with wave energy conservation, a relatively large decrease in the energy transmission speed in the long-period waves is compensated by the large increase in the wave height (Longuet-Higgins and Stewart, 1964), namely wave shoaling, resulting in the wave breaking with larger forces nearshore. Therefore, coastal regions where these waves reach would experience increasing sediment transport and coastal erosion (Rodriguez-Delgado et al., 2019). The wave breaking with increasing wave period transfers increasing momentum into the water column and elevates the mean sea level, potentially increasing coastal flooding.

The present study describes the mixed wave energy trends based on the Eulerian viewpoint of multi-wave systems passing the fixed location. In these complex wave climates, Lagrangian approaches, e.g., ray-tracing techniques, are required to further investigate physical mechanisms and sources of wave energy system changes. The implications of the results shown in the present study are limited to offshore applications because the global wave reanalysis data does not resolve nearshore wave physics, e.g., wave interactions and effects of bathymetric gradients, due to the coarse spatial resolution of the wave model. Nearshore high-resolution wave model hindcasts are needed to estimate nearshore regional wave energy climate changes and investigate the impacts of mixed wave energy trends on coastal applications, including coastal defenses to enhance community resilience against coastal hazards.

The historical changes in the global wave energy systems observed in the present study are derived from a single data source with the longest period of record available and using common statistical methods. Sensitivities and uncertainties in trend estimates from various wave data sources generated from different wave model setups need to be further investigated as the spectral partitioned wave data used in the present study is sensitive to wave model calibration and the spectral partitioning process. In addition, wave data with longer periods of record will be applied as the sources and periods of record of the available global wave hindcast will increase in the near future. The present study assumes that variations in estimating trends from common statistical methods are insignificant (Young et al., 2011). Additional sensitivity studies and uncertainties analysis will be applied, e.g., linear regression, Mann-Kendall test, Seasonal Kendall test, and Singular Spectrum Analysis, when more data sources are available. The mixed trends in the wave energy systems may vary in the future as the wave climate changes are nonstationary. The new approach developed in the present study can be applied to discern future wave energy climate trends under various carbon-reduction scenarios.

5. Conclusion

The present study introduces a new approach for investigating the historical trends in global wave energy systems and demonstrates that combinations of mixed opposing trends in distinct wave energy systems generated from different wind systems determine the global wave energy climate changes. Previous investigations simplified the wave energy climate changes by quantifying linear trends in the bulk wave parameters, viz., wave power and significant wave height, and documented that historical trends in the wave power were neutral or statistically not significant over half the global wave sites. In fact, 91 % of global wave sites have experienced significant wave climate changes where opposite trends in distinct wave energy systems have offset each other at 45 % of global wave sites and created the appearance of neutral trends. This new approach reveals the limitations of current low-fidelity estimates of wave energy climate changes based on bulk wave parameters.

The largest positive and negative trends in the wave power are observed in the south and northeastern Pacific Oceans where both short and long-period wave energy systems have increased and decreased, respectively. In the eastern equatorial Pacific Ocean, positive trends in short-period trade wind waves have offset negative trends in long-period Pacific westerly waves. Conversely, negative trends in local wind waves have balanced and neutralized the positive trends in long-period waves generated by remote wind systems in many oceans, which are currently known to have no significant wave power trends, e.g., northern Atlantic and southern Indian Oceans. While these results may differ depending on data sources and statistical methods, these results support the need for investigating long-term trends in wave energy systems.

The mixed trends in dominant wave energy systems have shifted the wave energy distributions and changed the characteristics of regional wave energy climates. These energy shifts induced by the opposing wave energy trends have increased the wave energy period in many oceans, which potentially increases risks of coastal erosion, flooding, and sea level rise. It also highlights the need to reassess ocean and coastal management policies and design practices for marine energy projects and infrastructure that assume a stationary wave climate.

CRediT authorship contribution statement

Seongho Ahn: Writing – original draft, Visualization, Validation, Methodology, Investigation, Formal analysis, Data curation, Conceptualization. **Vincent S. Neary:** Writing – review & editing, Supervision, Resources, Project administration, Investigation.

Declaration of competing interest

The authors declare that they have no known competing financial interests or personal relationships that could have appeared to influence the work reported in this paper.

Data availability

The authors do not have permission to share data.

Acknowledgment

The present study was supported by Sandia National Laboratories. Sandia National Laboratories is a multi-mission laboratory managed and operated by National Technology and Engineering Solutions of Sandia, LLC., a wholly owned subsidiary of Honeywell International, Inc., for the U.S. Department of Energy's National Nuclear Security Administration under contract DE-NA0003525. This paper describes objective technical results and analysis. Any subjective views or opinions that might be expressed in the paper do not necessarily represent the views of the U.S. Department of Energy or the United States Government. This research was supported by "Regional Innovation Strategy (RIS)" through the National Research Foundation of Korea (NRF) funded by the Ministry of Education (MOE) (2024RIS-009). This research was supported by Basic Science Research Program to Research Institute for Basic Sciences(RIBS) of Jeju National University through the National Research Foundation of Korea (NRF) funded by the Ministry of Education. (2019R1A6A1A10072987).

References

Aderinto, T., Li, H., 2019. Review on power performance and efficiency of wave energy converters. Energies 12, 1–24. https://doi.org/10.3390/en12224329.
Ahn, S., Haas, K.A., Neary, V.S., 2020. Dominant wave energy systems and conditional wave resource characterization for coastal waters of the United States. Energies 13, 3041. https://doi.org/10.3390/en13123041.
Ahn, S., Haas, K.A., Neary, V.S., 2019. Wave energy resource classification system for US coastal waters. Renew. Sustain. Energy Rev. 104, 54–68. https://doi.org/10.1016/j.rser.2019.01.017.
Ahn, S., Neary, V.S., 2021. Wave energy resource characterization employing joint distributions in frequency-direction-time domain. Appl. Energy 285, 116407. https://doi.org/10.1016/j.apenergy.2020.116407.
Ahn, S., Neary, V.S., 2020. Non-stationary historical trends in wave energy climate for coastal waters of the United States. Ocean Eng. 216, 108044. https://doi.org/10.1016/j.oceaneng.2020.108044.
Ahn, S., Neary, V.S., Allahdadi, M.N., He, R., 2021. Nearshore wave energy resource characterization along the East Coast of the United States. Renew. Energy. https://doi.org/10.1016/j.renene.2021.03.037.
Ahn, S., Neary, V.S., Ha, T., 2023. A practical method for modeling temporally-averaged ocean wave frequency-directional spectra for characterizing wave energy climates. Renew. Energy 207, 499–511. https://doi.org/10.1016/j.renene.2023.03.034.
Ahn, S., Neary, V.S., Haas, K.A., 2022. Global wave energy resource classification system for regional energy planning and project development. Renew. Sustain. Energy Rev. 162, 112438. https://doi.org/10.1016/j.rser.2022.112438.
Alexandrov, T., Bianconcini, S., Dagum, E.B., Maass, P., Mcelroy, T., Alexandrov, T., Bianconcini, S., Dagum, E.B., 2008. A review of some modern approaches to the problem of trend extraction. Econom. Rev. 31, 593–624. https://doi.org/10.1080/07474938.2011.608032.
Bidlot, J., 2020. Ocean Wave Model Output Parameters.
Casas-Prat, M., Hemer, M.A., Dodet, G., Morim, J., Wang, X.L., Mori, N., Young, I., Erikson, L., Kamranzad, B., Kumar, P., Menéndez, M., Feng, Y., 2024. Wind-wave climate changes and their impacts. Nat. Rev. Earth Environ. 5, 23–42. https://doi.org/10.1038/s43017-023-00502-0.
Chang, G., Jones, C.A., Roberts, J.D., Neary, V.S., 2018. A comprehensive evaluation of factors affecting the levelized cost of wave energy conversion projects. Renew. Energy 127, 344–354. https://doi.org/10.1016/j.renene.2018.04.071.
Christakos, K., Lavidas, G., Gao, Z., Björkqvist, J.V., 2024. Long-term assessment of wave conditions and wave energy resource in the Arctic Ocean. Renew. Energy 220, 119678. https://doi.org/10.1016/j.renene.2023.119678.
Cornett, A., 2008. A global wave energy resource assessment. In: International Offshore and Polar Engineering Conference. Canada. Vancouver.
Dallman, A.R., Neary, V.S., 2014. Characterization of U.S. Wave Energy Converter (WEC) Test Sites: A Catalogue of Met-Ocean Data. Albuquerque, NM, and Livermore, CA (United States). https://doi.org/10.2172/1160290.
De Leo, F., Briganti, R., Besio, G., 2024. Trends in ocean waves climate within the Mediterranean Sea: a review. Clim. Dynam. 62, 1555–1566. https://doi.org/10.1007/s00382-023-06984-4.
Dean, R.G., Dalrymple, R.A., 1991. Water Wave Mechanics for Engineers and Scientists, vol. 2. world scientific publishing company.
Dong, C., Huang, G., Cheng, G., Cai, Y., Chen, C., 2023. Macroscale altimetry-based estimation and analyses of wave power: a foundation of wave energy development over Canada. Renew. Sustain. Energy Rev. 183, 113469. https://doi.org/10.1016/j.rser.2023.113469.
Echevarria, E.R., Hemer, M.A., Holbrook, N.J., 2019. Seasonal variability of the global spectral wind wave climate. J. Geophys. Res. Ocean. 124, 2924–2939. https://doi.org/10.1029/2018JC014620.
Ghasemipour, N., Izanlou, P., Jahangir, M.H., 2022. Feasibility study on utilizing oscillating wave surge converters (OWSCs) in nearshore regions, case study: along the southeastern coast of Iran in Oman sea. J. Clean. Prod. 367, 133090. https://doi.org/10.1016/j.jclepro.2022.133090.
Goda, Y., 2010. Random Seas and Design of Maritime Structures Advanced Series on Ocean Engineering, vol. 33. World Scientific Publishing Ltd, p. 3rd.
Hand, M.M., Baldwin, S., DeMeo, E., Reilly, J.M., Mai, T., Arent, D., Porro, G., Meshek, M., Sandor, D., 2012. Renewable Electricity Futures Study. No. NREL/TP-6A20-52409).
Hansom, J.D., Switzer, A.D., Pile, J., 2014. Extreme waves: causes, characteristics, and impact on coastal environments and society. Coast. Mar. Hazards, Risks, Disasters 307–334. https://doi.org/10.1016/B978-0-12-396483-0.00011-X.
Hanson, J.L., Phillips, O.M., 2001. Automated analysis of ocean surface directional wave spectra. J. Atmos. Ocean. Technol. 18, 277–293. https://doi.org/10.1175/1520-0426(2001)018<0277:AAOOSD>2.0.CO;2.
Hersbach, H., Bell, B., Berrisford, P., Hirahara, S., Horányi, A., Muñoz-Sabater, J., Nicolas, J., Peubey, C., Radu, R., Schepers, D., Simmons, A., Soci, C., Abdalla, S., Abellan, X., Balsamo, G., Bechtold, P., Biavati, G., Bidlot, J., Bonavita, M., De Chiara, G., Dahlgren, P., Dee, D., Diamantakis, M., Dragani, R., Flemming, J., Forbes, R., Fuentes, M., Geer, A., Haimberger, L., Healy, S., Hogan, R.J., Hólm, E., Janisková, M., Keeley, S., Laloyaux, P., Lopez, P., Lupu, C., Radnoti, G., de Rosnay, P., Rozum, I., Vamborg, F., Villaume, S., Thépaut, J.N., 2020. The ERA5 global reanalysis. Q. J. R. Meteorol. Soc. 146, 1999–2049. https://doi.org/10.1002/qj.3803.
Hirsch, R.M., Slack, J.R., Smith, R.A., 1982. Techniques of trend analysis for monthly water quality data. Water Resour. Res. 18, 107–121. https://doi.org/10.1029/WR018i001p00107.
IEC, 2015. International Standard, Marine Energy – Wave, Tidal and Other Water Current Converters – Part 101: Wave Energy Resource Assessment and Characterization. IEC, Geneva, Switzerland, p. 62600, 101, Edition 1.0.
Méndez, F.J., Rueda, A., 2020. 3 - wave climates: deep water to shoaling zone. In: Jackson, D.W.T., Short, A.D. (Eds.), Sandy Beach Morphodynamics. Elsevier, pp. 39–59. https://doi.org/10.1016/B978-0-08-102927-5.00003-5.
Kendall, M.G., 1984. Rank Correlation Methods.
Kerkar, J.P., Seelam, J.K., 2024. Trends in the surface wind-wave heights in the North Indian Ocean based on 50-year NCEP/NCAR reanalysis wind-wave data. Reg. Stud. Mar. Sci. 72, 103430. https://doi.org/10.1016/j.rsma.2024.103430.
Kumar, N., Cahl, D.L., Crosby, S.C., Voulgaris, G., 2017. Bulk versus spectral wave parameters: implications on Stokes drift estimates, regional wave modeling, and HF radars applications. J. Phys. Oceanogr. 47, 1413–1431. https://doi.org/10.1175/JPO-D-16-0203.1.
Lemos, G., Semedo, A., Dobrynin, M., Behrens, A., Staneva, J., Bidlot, J.R., Miranda, P.M.A., 2019. Mid-twenty-first century global wave climate projections: results from a dynamic CMIP5 based ensemble. Global Planet. Change 172, 69–87. https://doi.org/10.1016/j.gloplacha.2018.09.011.
Longuet-Higgins, M.S., Stewart, R.W., 1964. Radiation stresses in water waves; a physical discussion, with applications. Deep Sea Res. Oceanogr. Abstr. 11, 529–562. https://doi.org/10.1016/0011-7471(64)90001-4.
Meucci, A., Young, I.R., Hemer, M., Trenham, C., Watterson, I.G., 2023. 140 Years of global ocean wind-wave climate derived from CMIP6 ACCESS-CM2 and EC-earth3 GCMs: global trends, regional changes, and future projections. J. Clim. 36, 1605–1631. https://doi.org/10.1175/JCLI-D-21-0929.1.
Mohamad, A., Alinejad-Tabrizi, T., Kavianpour, M., Shamshirband, S., 2020. Projection of spatiotemporal variability of wave power in the Persian Gulf by the end of 21st century: GCM and CORDEX ensemble. J. Clean. Prod. 256, 120400. https://doi.org/10.1016/j.jclepro.2020.120400.
National Oceanic and Atmospheric Administration, 2020. WAVEWATCH III® hindcast and reanalysis archives [WWW Document]. Natl. Ocean. Atmos. Adm. URL. http://polar.ncep.noaa.gov/waves/hindcasts/.
Prendergast, J., Li, M., Sheng, W., 2020. A study on the effects of wave spectra on wave energy conversions. IEEE J. Ocean. Eng. 45, 271–283. https://doi.org/10.1109/JOE.2018.2869636.
Reguero, B.G., Losada, I.J., Méndez, F.J., 2019. A recent increase in global wave power as a consequence of oceanic warming. Nat. Commun. 10, 1–14. https://doi.org/10.1038/s41467-018-08066-0.
Reguero, B.G., Losada, I.J., Méndez, F.J., 2015. A global wave power resource and its seasonal, interannual and long-term variability. Appl. Energy 148, 366–380. https://doi.org/10.1016/j.apenergy.2015.03.114.
Rodriguez-Delgado, C., Bergillos, R.J., Iglesias, G., 2019. Dual wave farms for energy production and coastal protection under sea level rise. J. Clean. Prod. 222, 364–372. https://doi.org/10.1016/j.jclepro.2019.03.058.
Romano-Moreno, E., Diaz-Hernandez, G., Tomás, A., Lara, J.L., 2023. Multimodal harbor wave climate characterization based on wave agitation spectral types. Coast. Eng. 180. https://doi.org/10.1016/j.coastaleng.2022.104271.
Rusu, L., 2019. Evaluation of the near future wave energy resources in the Black Sea under two climate scenarios. Renew. Energy 142, 137–146. https://doi.org/10.1016/j.renene.2019.04.092.
Rusu, L., Rusu, E., 2021. Evaluation of the worldwide wave energy distribution based on ERA5 data and altimeter measurements. Energies 14. https://doi.org/10.3390/en14020394.
Shi, J., Feng, X., Toumi, R., Zhang, C., Hodges, K.I., Tao, A., Zhang, W., Zheng, J., 2024. Global increase in tropical cyclone ocean surface waves. Nat. Commun. 15. https://doi.org/10.1038/s41467-023-43532-4.

Sun, P., Xu, B., Wang, J., 2022. Long-term trend analysis and wave energy assessment based on ERA5 wave reanalysis along the Chinese coastline. Appl. Energy 324, 119709. https://doi.org/10.1016/j.apenergy.2022.119709.

Timmermann, A., McGregor, S., Jin, F.F., 2010. Wind effects on past and future regional sea level trends in the southern Indo-Pacific. J. Clim. 23, 4429–4437. https://doi.org/10.1175/2010JCLI3519.1.

Timmermans, B.W., Gommenginger, C.P., Dodet, G., Bidlot, J.R., 2020. Global wave height trends and variability from new multimission satellite altimeter products, reanalyses, and wave buoys. Geophys. Res. Lett. 47. https://doi.org/10.1029/2019GL086880.

Vitousek, S., Barbee, M.M., Fletcher, C.H., Richmond, B.M., Genz, A.S., 2009. Coastal Hazard Analysis Report, Coastal Hazard Analysis Report.

Wang, J., Wang, Y., 2022. Evaluation of the ERA5 significant wave height against NDBC buoy data from 1979 to 2019. Mar. Geodesy 45, 151–165. https://doi.org/10.1080/01490419.2021.2011502.

Yang, Z., García, G., Neary, V.S., Ahn, S., Kilcher, L., Bharath, A., 2023. Multi-decade high-resolution regional hindcasts for wave energy resource characterization in U . S . coastal waters. Renew. Energy 212, 803–817. https://doi.org/10.1016/j.renene.2023.03.100.

Young, I.R., Ribal, A., 2019. Multiplatform evaluation of global trends in wind speed and wave height. Science 364, 548–552. https://doi.org/10.1126/science.aav9527.

Young, I.R., Zieger, S., Babanin, A.V., 2011. Global trends in wind speed and wave height. Science 332, 451–456.

Zheng, C., wei, Li, hong, X., Azorin-Molina, C., Li, C. yin, Wang, Q., Xiao, Z. niu, Yang, S. bo, Chen, X., Zhan, C., 2022. Global trends in oceanic wind speed, wind-sea, swell, and mixed wave heights. Appl. Energy 321. https://doi.org/10.1016/j.apenergy.2022.119327.

Zhou, J., Zhang, H., Li, P., Lu, Y., Xu, D., 2023. High efficiency and wideband wave energy capture of a bistable wave energy converter with a displacement amplifier. J. Clean. Prod. 429, 139654. https://doi.org/10.1016/j.jclepro.2023.139654.